

# Eph signaling is required for segmentation and differentiation of the somites

Lindsey Durbin,<sup>1</sup> Caroline Brennan,<sup>1</sup> Kensuke Shiomi, Julie Cooke, Arantza Barrios, Shantha Shanmugalingam, Brenda Guthrie,<sup>3</sup> Rick Lindberg,<sup>2</sup> and Nigel Holder<sup>3</sup>

Department of Anatomy and Developmental Biology, University College, London, WC1E 6BT, UK; <sup>2</sup>Amgen Center, Thousand Oaks, California 91320 USA

**Somitogenesis involves the segmentation of the paraxial mesoderm into units along the anteroposterior axis. Here we show a role for Eph and ephrin signaling in the patterning of presomitic mesoderm and formation of the somites. *Ephrin-A-L1* and *ephrin-B2* are expressed in an iterative manner in the developing somites and presomitic mesoderm, as is the Eph receptor *EphA4*. We have examined the role of these proteins by injection of RNA, encoding dominant negative forms of Eph receptors and ephrins. Interruption of Eph signaling leads to abnormal somite boundary formation and reduced or disturbed *myoD* expression in the myotome. Disruption of Eph family signaling delays the normal down-regulation of *her1* and *Delta D* expression in the anterior presomitic mesoderm and disrupts myogenic differentiation. We suggest that Eph signaling has a key role in the translation of the patterning of presomitic mesoderm into somites.**

[Key Words: Somitogenesis; Eph/ephrin signaling; zebrafish]

Received March 5, 1998; revised version accepted July 10, 1998.

The subdivision of paraxial mesoderm into somites is the initial mesodermal segmentation event of vertebrate development. The formation and differentiation of somites is the result of three distinct processes: pre-patterning of the mesoderm, boundary formation, and patterning within the somite itself. Several lines of evidence suggest that the presomitic mesoderm is prepatterned into metameric subunits (Gossler and Hrabe de Angelis 1998). Recently, molecular evidence for segmental subdivision of the presomitic mesoderm has been obtained. The basic helix-loop-helix (bHLH) transcription factors *her1* and *c-hairy-1* are expressed dynamically in the pre-segmental somitic plate of zebrafish and chick, respectively (Muller et al. 1996; Palmeirim et al. 1997). Their expression patterns suggest that these genes function in the establishment of a segmental pattern within this region of the embryo, although it is not clear at this stage whether these genes function in the same way. The transcription factor *MesP2* is also required for normal segmentation (Saga et al. 1997). The second process of somite development involves the translation of the segmental prepattern into the morphogenetic changes that accompany formation of the somite boundaries. Recently a number of studies have shown that Notch-Delta intercellular signaling is involved in boundary for-

mation; altering the function of Notch or Delta by loss and gain of function leads to abnormal somite formation. Finally, the somites themselves are patterned and differentiation events take place (Gossler and Hrabe de Angelis 1998).

Intercellular signaling is one of the processes that underlies segmentation in vertebrate embryos. The Eph family of receptor tyrosine kinases are cell surface molecules shown to have a role in intercellular signaling and patterning of the neural tube (Gale and Yancopoulos 1997). Several Eph receptors and ephrins are expressed in the somites (Bergemann et al. 1995; Scales et al. 1995; Flenniken et al. 1996; Gale et al. 1996; Cooke et al. 1997). Ephrins can be divided into two classes according to their method of membrane attachment; class A ephrins have a glycosyl-phosphatidylinositol (GPI) linkage and class B ephrins are transmembrane proteins capable of transducing a signal into the expressing cell (Holland et al. 1996; Bruckner et al. 1997). Eph receptors can also be divided into two classes according to their binding preferences such that EphA receptors bind class A ephrins, whereas EphB receptors recognize class B ephrins. Several groups have demonstrated that in vitro binding within these classes is promiscuous and any class A receptor can bind any class A ephrin (Brambilla et al. 1995; Gale et al. 1996). Using injections of RNA encoding full-length or truncated forms of EphA4 into zebrafish eggs we have demonstrated a role for the Eph family in hind-brain segmentation and forebrain patterning (Xu et al.

<sup>1</sup>These authors contributed equally to the work.

<sup>3</sup>Corresponding author.

E-MAIL N.Holder@ucl.ac.uk; FAX 0171-504-2091.

1995, 1996). A similar approach has been used to demonstrate the role of the Eph family in neural crest migration in *Xenopus* (Smith et al. 1997). As binding is promiscuous between different members of the same subclass, high level ectopic expression of a dominant negative form of a class A protein would be expected to interfere with signaling to all class A receptors. This could be achieved by the ability of the dominant negative receptor to bind to endogenous type A ligands, preventing them from binding to endogenous receptor, or by heterodimerization. As soluble forms of ephrins can bind receptors but do not cause activation, these act as receptor antagonists (Krull et al. 1997). Thus, injection of RNA to encode dominant negative forms of a class A and class B receptor and a soluble class A and class B ephrin will give an indication of the role of the Eph family in any particular developmental process.

We have isolated a class A ligand of uncertain homology, *ephrin-A-L1*, and *ephrin-B2* in zebrafish and we demonstrate here their expression in the somites. We injected RNA encoding soluble forms of these ligands and dominant negative forms of the class A receptor EphA4 and a class B receptor of uncertain homology EphB-rtk8 (Cooke et al. 1997) to investigate the role of the Eph family in somite development. We show that disruption of Eph signaling results in the abnormal formation of somite boundaries.

## Results

### *Cloning of zebrafish ephrin class A ligand L1, ephrin-B2, and Eph class B receptor rtk8*

Fragments of the two ligands *ephrin-A-L1* and *ephrin-B2* were isolated by PCR amplification of a zebrafish neurula stage cDNA library. The degenerate primers used for the PCR were complimentary to conserved regions within *ephrin-A1* (Bartley et al. 1994) and *ephrin-A5* (Winslow et al. 1995) for *ephrin-A-L1*, and *ephrin-B2* (Bergemann et al. 1995) and *ephrin-B1* (Fletcher et al. 1994) for *ephrin-B2*. cDNAs containing complete open reading frames were isolated for these ephrins by screening the neurula stage cDNA library with the PCR fragments. Sequence comparisons showed both *ephrin-A-L1* and *ephrin-B2* to contain the four conserved cysteine residues in the putative receptor-binding region characteristic of the ephrin family. *Ephrin-A-L1* also has a GPI linkage signal indicating that this is a class A ephrin, and *ephrin-B2* has a transmembrane domain showing that this is a class B ephrin (Fig. 1). *Ephrin-A-L1* is not necessarily the ortholog of any higher vertebrate ephrin, but it shows most homology to ephrin-A1 (59% similar and 48% identical at the amino acid level). Zebrafish ephrin-B2 is 66% identical to and 83% similar to mouse ephrin-B2 at the amino acid level.

The full-length *EphB-rtk8* coding region was isolated by screening a zebrafish 3–15 hr cDNA library with a fragment from a previously isolated *EphB-rtk8* partial cDNA (Cooke et al. 1997; Fig. 1). It is not possible to determine the higher vertebrate ortholog of *EphB-rtk8*,

although it shows greatest homology to EphB4 (60% identical and 70% similar at the amino acid level).

### *Ephrin-A-L1, ephrin-B2, and EphA4 are expressed in the somites as they form*

The expression patterns of *ephrin-A-L1* and *ephrin-B2* were investigated by in situ hybridization, and both are expressed in the somites as they are formed (Fig. 2). *Ephrin-B2* expression is first seen in the germ ring of 30%–60% epiboly embryos (Fig. 2A). In bud stage embryos *ephrin-B2* transcripts are detected in three stripes in the paraxial mesoderm, and in a stripe in the presumptive hindbrain (Fig. 2B), and other regions of the anterior neural plate (data not shown). At the two-somite stage four stripes of *ephrin-B2* expression are seen in the paraxial mesoderm, two of which are in the presomitic mesoderm (Fig. 2C), and in the tailbud. By six somites, *ephrin-B2* is expressed in the posterior region of the formed somites and in two or three stripes in the rostral presomitic mesoderm. These presomitic expression domains correspond to posterior domains of the most rostral presumptive somites (Fig. 2D). As the somites differentiate, the anteroposterior restriction of *ephrin-B2* expression is lost, and *ephrin-B2* is found in a lateral domain. From 16 somites *ephrin-B2* expression is further restricted to dorsal and ventral lateral regions within the most anterior somites. From 24 somites loss of *ephrin-B2* expression is initiated in an anterior to posterior wave. By prim-5 (24 hr after fertilization) only the most posterior somites still express *ephrin-B2*.

Expression of *ephrin-A-L1* is first seen at 60%–70% epiboly in the epibolizing margin and in the hypoblast. Expression is higher on the ventral than the dorsal side of the embryo (Fig. 2E). At 90%–100% epiboly *ephrin-A-L1* is still detected around the margin with stronger expression on the dorsal side in the presumptive tailbud and with weak expression in cells on either side of the presumptive notochord (Fig. 2F). Between the one- and five-somite stages *ephrin-A-L1* transcripts are detected in the tailbud and adaxial cells and weakly in stripes in the somitic mesoderm and throughout the most rostral presomitic mesoderm (Fig. 2G). During these stages *ephrin-A-L1* expression is also detected in individual paired cells in the neural tube and around the pillow. From the six-somite stage *ephrin-A-L1* is expressed more strongly in the posterior region of the formed somites (Fig. 2H). After the completion of somitogenesis *ephrin-A-L1* expression is lost progressively in an anterior-to-posterior wave in a similar fashion to that seen with *ephrin-B2*.

Because several members of the Eph family in zebrafish and other species are expressed in the somites we investigated the expression of the other known zebrafish members of the Eph family in the somites and the presomitic mesoderm. The expression of three other Eph ligands (*ephrin-A-L2*, *ephrin-A-L3*, and *ephrin-A-L4*; Brennan et al. 1997; Macdonald et al. 1997) and nine receptors (*Eph-rtk 1–8*, and *EphA-Zdk*; Xu et al. 1994; Taneja et al. 1996; Cooke et al. 1997) was determined by in situ hybridization during gastrula and somite stages.

**A**

ephrin-A-L1	1	MDFLWLLCVA	VSVSANYASA	ERHSVYWNST	NANFLWDDYT	VDVRINDYLD	50
	51	II <sup>C</sup> PHYAHGE	IASQEAERYV	LYMVELEDYE	NCKPHSFDQL	RWEC <sup>S</sup> SRFPAP	100
	101	HAPEKFSSEK	QRFTPTFLGK	EFRQGSESYV	ISKPLHHHGQ	E <sup>C</sup> LRLLKVDVV	150
	151	GPHGSKNKKK	MVEKVEEIEG	KMAAGGVHNP	SNRLPADDDI	AMIPV <sup>V</sup> VQRSV	200
	201	GSSGVSVAPI	SSFVTLLESVF	ICLVLHQAS			229

**B**

zebrafish ephrin-B2	1	MG-----DS	LWRVYFGVIV	IACKVNL <sup>S</sup> RA	LILDSIY <sup>W</sup> NT	TNTRFVPG <sup>Q</sup> Q	44
mouse ephrin-B2	1	MAMARSRRDS	VWRYCGGLM	VLCRTAISRS	IVLEPIY <sup>W</sup> NS	SNSKFLPG <sup>Q</sup> Q	50
human ephrin-B2	1	MAV---RRDS	VWRYCGGLM	VLCRTAISRS	IVLEPIY <sup>W</sup> NS	SNSKFLPG <sup>Q</sup> Q	47

zebrafish ephrin-B2	45	LVLVY <sup>P</sup> QIGDK	MDIV <sup>E</sup> PRVEG	GSMEGV <sup>E</sup> YK	LYM <sup>V</sup> PLEQLK	SC <sup>O</sup> VTKADTP	94
mouse ephrin-B2	51	LVLVY <sup>P</sup> QIGDK	EDIV <sup>E</sup> PRVDS	KTVGQ <sup>V</sup> EYK	VYM <sup>V</sup> DKDQAD	R <sup>C</sup> TIKKENTP	100
human ephrin-B2	48	LVLVY <sup>P</sup> QIGDK	EDIV <sup>E</sup> PRVDS	KTVGQ <sup>V</sup> EYK	VYM <sup>V</sup> DKDQAD	R <sup>C</sup> TIKKENTP	97

zebrafish ephrin-B2	95	LLN <sup>C</sup> AKPKDQ	VKFTL <sup>K</sup> FOEF	SPNLWGLEFF	RGKDY <sup>I</sup> IIST	SNGTMEGLDN	144
mouse ephrin-B2	101	LLN <sup>C</sup> AKPKDQ	VKFTL <sup>K</sup> FOEF	SPNLWGLEFF	RKNDY <sup>I</sup> IIST	SNGSLEGLDN	150
human ephrin-B2	98	LLN <sup>C</sup> AKPKDQ	IKFTL <sup>K</sup> FOEF	SPNLWGLEFF	RKNDY <sup>I</sup> IIST	SNGSLEGLDN	147

zebrafish ephrin-B2	145	OEGGV <sup>C</sup> QTKS	MKILMKV <sup>Q</sup> Q	PSDPI <sup>S</sup> FKDY	-P <sup>T</sup> SYPPKHP	DLGGK <sup>D</sup> KSN	193
mouse ephrin-B2	151	OEGGV <sup>C</sup> QTRA	MKILMKV <sup>Q</sup> Q	ASSAGS <sup>A</sup> RNH	GP <sup>T</sup> RRPELEA	GTNGRS <sup>S</sup> TS	200
human ephrin-B2	148	OEGGV <sup>C</sup> QTRA	MKILMKV <sup>Q</sup> Q	ASSAGS <sup>A</sup> TRNK	D <sup>P</sup> TRRPELEA	GTNGRS <sup>S</sup> TS	197

zebrafish ephrin-B2	194	EVLKPDASPH	GEDKGDG <sup>N</sup> KS	SSVIGSEVAL	FACIASASVI	VIIIIIMLV <sup>F</sup>	243
mouse ephrin-B2	201	PFVKPNP <sup>G</sup> SS	TDGNSAG <sup>H</sup> SG	NNLLGSEVAL	FAGIASG <sup>C</sup> II	PIV <sup>I</sup> IITLVV	250
human ephrin-B2	198	PFVKPNP <sup>G</sup> SS	TDGNSAG <sup>H</sup> SG	NNLLGSEVAL	FAGIASG <sup>C</sup> II	PIV <sup>I</sup> IITLVV	247

zebrafish ephrin-B2	244	LLLKY <sup>R</sup> RRHR	KHSPO <sup>H</sup> HTTL	SLSTL <sup>A</sup> T <sup>P</sup> RR	GGSGGN <sup>N</sup> NGS	EPSDII <sup>I</sup> PLR	293
mouse ephrin-B2	251	LLLKY <sup>R</sup> RRHR	KHSPO <sup>H</sup> HTTL	SLSTL <sup>A</sup> T <sup>P</sup> RR	GG---NN <sup>N</sup> GS	EPSDII <sup>I</sup> PLR	297
human ephrin-B2	248	LLLKY <sup>R</sup> RRHR	KHSPO <sup>H</sup> HTTL	SLSTL <sup>A</sup> T <sup>P</sup> RR	SG---NN <sup>N</sup> GS	EPSDII <sup>I</sup> PLR	294

zebrafish ephrin-B2	294	TADSV <sup>F</sup> CPHY	EKVS <sup>G</sup> DYGH <sup>P</sup>	VYIVQ <sup>E</sup> MP <sup>P</sup> Q	SPANI <sup>Y</sup> YKV		333
mouse ephrin-B2	298	TADSV <sup>F</sup> CPHY	EKVS <sup>G</sup> DYGH <sup>P</sup>	VYIVQ <sup>E</sup> MP <sup>P</sup> Q	SPANI <sup>Y</sup> YKV		337
human ephrin-B2	295	TADSV <sup>F</sup> CPHY	EKVS <sup>G</sup> DYGH <sup>P</sup>	VYIVQ <sup>E</sup> MP <sup>P</sup> Q	SPANI <sup>Y</sup> YKV		334

**C**

EphB-rtk 8	1	MDRV <sup>C</sup> WIMAL	SWF <sup>W</sup> MYSTGL	VSAEE <sup>E</sup> VL <sup>M</sup> N	TKLETSD <sup>L</sup> LRW	TIYPSG <sup>D</sup> PEW	50
	51	EEMSG <sup>L</sup> DEEG	NSVRT <sup>F</sup> QV <sup>Q</sup> P	MDSSV <sup>S</sup> H <sup>W</sup> LR	TRFIP <sup>R</sup> HGAS	QVYVEI <sup>R</sup> FTM	100
	101	ME <sup>C</sup> SAMPAS <sup>F</sup>	RI <sup>C</sup> KET <sup>F</sup> NLY	YYQSD <sup>E</sup> D <sup>T</sup> AS	ATHPAW <sup>M</sup> ENP	YSKV <sup>D</sup> TVAAD	150
	151	FLRRG <sup>G</sup> GERK	SNVKT <sup>V</sup> RV <sup>G</sup> P	LSLFG <sup>F</sup> Y <sup>L</sup> AF	QTQGA <sup>C</sup> MALL	SVRV <sup>F</sup> FK <sup>C</sup> P	200
	201	AVSRA <sup>F</sup> SSFP	ETLPH <sup>S</sup> LV <sup>Q</sup> Q	AEGV <sup>C</sup> VD <sup>N</sup> SA	PTG <sup>Q</sup> C <sup>T</sup> APPT	M <sup>F</sup> QGED <sup>G</sup> QVW	250
	251	GPFS <sup>T</sup> Q <sup>A</sup> CK	PGYEP <sup>V</sup> DS <sup>D</sup> R	CRAC <sup>G</sup> LG <sup>Q</sup> YK	ASVGS <sup>L</sup> CR <sup>V</sup>	CPD <sup>N</sup> SNT <sup>H</sup> SA	300
	301	GSSLC <sup>V</sup> CRFG	YHRAT <sup>S</sup> DL <sup>F</sup> D	SA <sup>C</sup> TK <sup>F</sup> PS <sup>A</sup> P	RSIIY <sup>Q</sup> IND <sup>T</sup>	VVTL <sup>E</sup> WSE <sup>P</sup> L	350
	351	DRGGR <sup>S</sup> DL <sup>S</sup> Y	SVE <sup>C</sup> M <sup>C</sup> RG <sup>S</sup>	LV <sup>Q</sup> QCAD <sup>S</sup> IT	YRPG <sup>Q</sup> MV <sup>S</sup> G	RRVI <sup>R</sup> IG <sup>L</sup> LP	400
	401	HTTY <sup>T</sup> FT <sup>V</sup> LA	QNGV <sup>S</sup> AV <sup>S</sup> HT	SPASS <sup>S</sup> V <sup>N</sup> IT	TSRD <sup>V</sup> AV <sup>P</sup> VS	GIR <sup>R</sup> KASE <sup>S</sup>	450
	451	SVSIS <sup>W</sup> T <sup>V</sup> PP	QTQHS <sup>I</sup> Q <sup>D</sup> YQ	LYSLK <sup>G</sup> Q <sup>D</sup> D	GWQY <sup>S</sup> SR <sup>S</sup> S	SVV <sup>L</sup> ND <sup>L</sup> SR <sup>A</sup>	500
	501	SQY <sup>Q</sup> VQ <sup>V</sup> RR	TAAGY <sup>G</sup> H <sup>F</sup> SS	AVSIS <sup>T</sup> L <sup>P</sup> DD	EES <sup>P</sup> SR <sup>L</sup> ML <sup>T</sup>	GVL <sup>V</sup> AIG <sup>L</sup> LI	550
	551	L <sup>L</sup> AV <sup>V</sup> IV <sup>A</sup> VF	CFRR <sup>S</sup> TR <sup>R</sup> RD	PD <sup>P</sup> DK <sup>S</sup> G <sup>Q</sup> FL	MGQ <sup>G</sup> IK <sup>V</sup> Y <sup>I</sup> D	PFT <sup>Y</sup> ED <sup>P</sup> NEA	600
	601	VREF <sup>A</sup> KEID <sup>V</sup>	S <sup>F</sup> V <sup>K</sup> IEE <sup>V</sup> IG	AGE <sup>F</sup> G <sup>V</sup> EC <sup>R</sup> G	RLK <sup>V</sup> PG <sup>K</sup> EN	YVA <sup>I</sup> KT <sup>L</sup> K <sup>G</sup> G	650
	651	YTDK <sup>R</sup> RR <sup>D</sup> FL	SEAS <sup>I</sup> MG <sup>Q</sup> FQ	HPNI <sup>H</sup> LE <sup>G</sup> V	ITASC <sup>P</sup> V <sup>M</sup> LL	TEY <sup>M</sup> ENG <sup>A</sup> LD	700
	701	SFL <sup>R</sup> ND <sup>G</sup> QF	TRI <sup>Q</sup> L <sup>V</sup> GM <sup>L</sup> R	GIAS <sup>G</sup> M <sup>K</sup> Y <sup>L</sup> S	EMSF <sup>V</sup> HR <sup>D</sup> LA	ARN <sup>I</sup> L <sup>V</sup> NS <sup>N</sup> L	750
	751	VCKV <sup>S</sup> DF <sup>G</sup> LS	RFL <sup>T</sup> ENS <sup>S</sup> DP	TYT <sup>S</sup> SL <sup>G</sup> CKI	PIRW <sup>T</sup> APE <sup>A</sup> I	AFR <sup>K</sup> T <sup>S</sup> AS <sup>D</sup>	800
	801	VMSY <sup>G</sup> IV <sup>M</sup> VE	VMS <sup>F</sup> GER <sup>P</sup> YW	DMS <sup>N</sup> Q <sup>D</sup> V <sup>I</sup> NA	IEQ <sup>D</sup> Y <sup>R</sup> L <sup>P</sup> PP	PEC <sup>P</sup> AS <sup>L</sup> H <sup>Q</sup> L	850
	851	MLDC <sup>W</sup> Q <sup>K</sup> ERS	SRPR <sup>F</sup> CA <sup>I</sup> VS	ALD <sup>R</sup> L <sup>R</sup> IN <sup>P</sup> FA	SLK <sup>I</sup> T <sup>G</sup> RI <sup>P</sup> D	GPS <sup>H</sup> PL <sup>L</sup> D <sup>Q</sup> R	900
	901	APP <sup>L</sup> SH <sup>C</sup> SS	VAD <sup>W</sup> L <sup>R</sup> AI <sup>K</sup> M	ERYE <sup>D</sup> AF <sup>M</sup> QA	GFT <sup>A</sup> I <sup>Q</sup> H <sup>I</sup> TH	ISTE <sup>D</sup> LL <sup>R</sup> IG	950
	951	VTLAG <sup>H</sup> Q <sup>K</sup> KI	LSSV <sup>Q</sup> TL <sup>R</sup> I <sup>H</sup>	GGSL <sup>R</sup> Y			976

**Figure 1.** (A) Amino acid sequence of zebrafish ephrin-A-L1. (B) Alignment of the protein sequences of zebrafish ephrin-B2 with mouse and human ephrin-B2. Identical residues shown by shading. (C) Amino acid sequence of zebrafish EphB-rtk8. Signal sequences are underlined; probable transmembrane domains are double underlined; putative GPI linkage signal is overlined; conserved cysteine residues are boxed.

Of the receptors examined only *EphA4* expression is detected in the presomitic mesoderm and forming somites throughout somitogenesis. Transcripts for *EphA4* are first detected in the region of the somites in one-somite stage embryos. At this stage a stripe of expression in a position corresponding to the somite boundary is seen (Fig. 2I). In three-somite embryos four or five stripes of *EphA4* expression can be detected in the presomitic and somitic mesoderm. The most posterior of these expression domains corresponds to anterior domains within the anterior presumptive somites (Fig. 2J and Fig. 7A, below). The other stripes of expression correspond to domains in the anterior of the somites that have already formed. *EphA4* is strongly expressed in the adaxial cells during early somite stages, and is detected throughout the posterior paraxial mesoderm.

Of the nine receptors and five ligands studied only *ephrin-A-L1*, *ephrin-B2*, and *EphA4* were detected in a segmental pattern in the presomitic mesoderm. The spatially restricted expression of these genes within the presomitic mesoderm is suggestive of a role in somite formation. The expression of *ephrin-B2* and *EphA4* in the presomitic mesoderm is indicative of an anteroposterior prepattern within the presumptive somite.

*Ephrin-B2 binds to EphB-rtk8 and EphA4, whereas ephrin-A-L1 binds to EphA4 but not EphB-rtk8*

Before functional studies we assessed the binding characteristics of ephrin-A-L1, ephrin-B2, and EphA4. Fusions of Eph family members with alkaline phosphatase (AP) were used to investigate the binding of these pro-

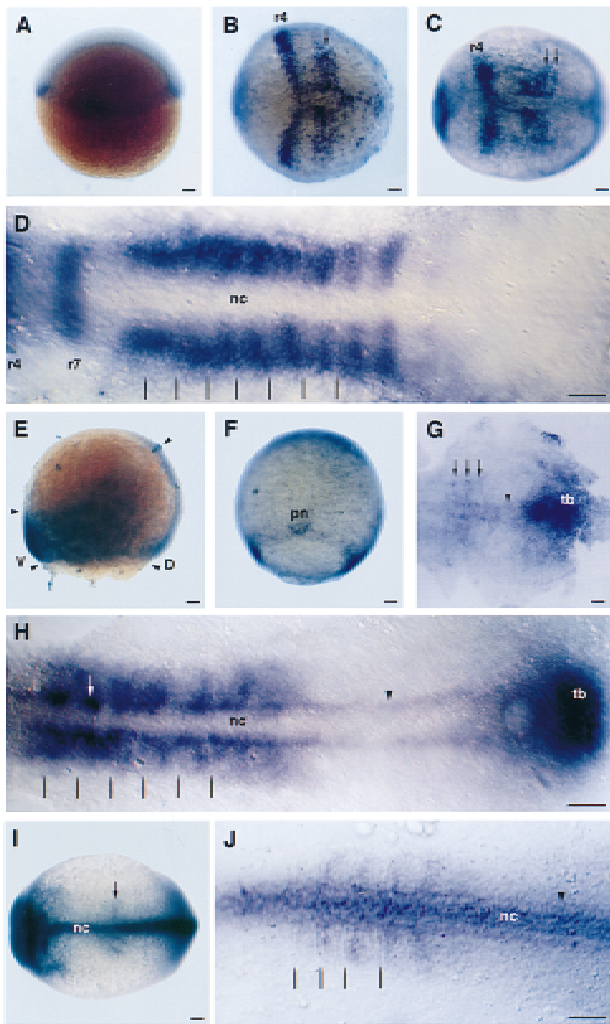


**Figure 2.** Expression of *ephrin-B2* (A–D), *ephrin-A-L1* (E–H), and *EphA4* (I,J). Embryos were hybridized with digoxigenin-labeled antisense RNA probes. Dorsal views (except E lateral view), anterior is to the left (except in A, E,F where anterior is to the top). *ephrin-B2* expression. (A) 50% epiboly. Transcripts are detected around the germ ring. (B) Bud stage. Expression is seen in presumptive rhombomere 4 and in three stripes in the presomitic mesoderm (arrow). (C) Two somites. Transcripts are detected in rhombomere 4, in the somites, and in two stripes in the anterior presomitic mesoderm (arrows). (D) Six somites. Expression is seen in rhombomeres 4 and 7, in a posterior domain of the formed somites and in a posterior domain of the most anterior presumptive somites (lines mark the somite boundaries). *ephrin-B2* expression is restricted to a lateral domain within the somites as these mature. *Ephrin-A-L1* expression. (E) 70% epiboly. Transcripts are detected in the epibolizing margin and the hypoblast, expression is stronger on the ventral side of the embryo (arrowheads mark the edges of the expression domain). (F) 90% epiboly. Expression is seen in the epibolizing margin, more strongly around the tailbud, and in cells on either side of the presumptive notochord. (G) One somite. Transcripts are detected in the tailbud, adaxial cells (arrowhead), and in three weak stripes in the formed somite and anterior presomitic mesoderm (arrows). (H) Six somites. Expression is seen in the tailbud and adaxial cells (arrowhead). *Ephrin-A-L1* is expressed throughout the somites and anterior presomitic mesoderm, more strongly in the posterior region of each segment (lines mark the somite boundaries). Transcripts are also detected in individual paired cells in the neural tube (white arrow). *EphA4* expression. (I) One somite. Transcripts are detected in the notochord and adaxial cells, and in one stripe in the formed somite (arrow). (J) Three somites. Expression is seen in the notochord and adaxial cells (arrowhead), and in an anterior domain of the somites and most anterior presumptive somites (lines mark the somite boundaries). (D) dorsal; (nc) notochord; (pn) presumptive notochord; (r) rhombomere; (tb) tailbud; (V) ventral; Bars, 100  $\mu$ m.

teins in vitro in cell culture and in embryos. Ephrin-A-L1-AP bound to Cos cells transfected with EphA4, but did not bind to cells transfected with EphB-rtk8 (Fig. 3A,B). Ephrin-B2-AP bound to cells transfected with either EphB-rtk8 or EphA4 (Fig. 3C,D), a result consistent with the binding characteristics of mouse EphA4, which has been shown previously to bind to B class as well as A class ephrins (Gale et al. 1996). Both EphA4 and EphB-rtk8 are capable of binding to ephrin-B2, which is strongly expressed in the presumptive somites from as early as 100% epiboly. Overexpression of dominant negative constructs of either of these genes would be expected to interfere with ephrin-B2 function in this area of the embryo. EphA4 but not EphB-rtk8 is capable of binding to ephrin-A-L1 and dominant negative forms of EphA4 would also interfere with signaling mediated through this ligand.

Because of the promiscuity of binding shown by members of the Eph family, AP fusion proteins used on embryos find all unbound receptor or ligand molecules of the appropriate class (Gale et al. 1996). To determine whether ligands bound to domains in which no known

receptors are expressed, or vice versa, we determined the in situ pattern of representative AP fusion proteins for each ligand and receptor class. The class B receptor AP protein (EphB-rtk8-AP) gave a binding pattern within the somites with similar temporal and spatial characteristics as *ephrin-B2* expression (Fig. 3G). The class A receptor-AP (EphA-rtk6-AP) gave a binding pattern within the presomitic mesoderm and somites of 95% epiboly to six-somite stage embryos with similar onset and spatial characteristics as *ephrin-A-L1* expression (Fig. 3E,F). Neither the class A (ephrin-A-L4-AP, ephrin-A-L3-AP, or ephrin-A-L1-AP) nor the class B (ephrin-B2-AP) ligand AP fusion proteins show any binding in the somites above background levels, despite giving specific binding patterns in other regions of the embryo consistent with the known expression profiles of Eph family receptors. It would be predicted from in vitro-binding studies that both the class A and B ephrin-AP proteins would recognize and bind to any available EphA4 in the forming somites. However, the expression of *EphA4* in this region is much weaker than in the axial mesoderm or neuroectoderm (Fig. 2I,J), and also weaker than the

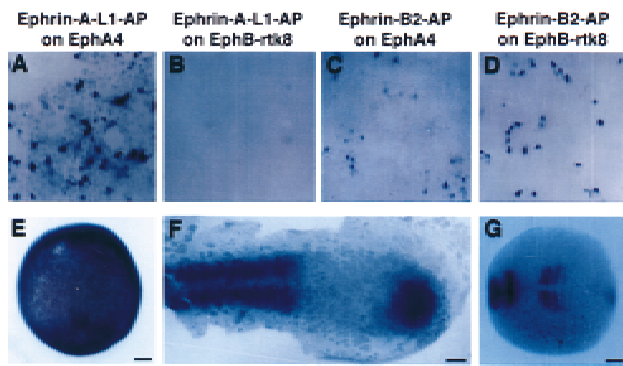


**Figure 3.** Analysis of the binding characteristics of Eph family proteins in vitro and in situ using alkaline phosphatase-tagged proteins. (A–D) The in vitro binding characteristics of ephrin-A-L1 (A,B) and ephrin-B2 (C,D). Ephrin-B2-AP and ephrin-A-L1-AP were put on Cos cells that had been transfected with EphA4 (A,C) or EphB-rtk8 (B,D). Staining of cells indicates that the ligand binds to the expressed receptor. Both ephrin-A-L1 and ephrin-B2 can bind to EphA4 (A,C), but only ephrin-B2 can bind to EphB-rtk8 (B,D). The presence of class A and B ephrins within the somites was investigated in situ using an AP-tagged protein representative for each of the receptor classes. Dorsal views, anterior is to the *left* (except in *E* where anterior is to the *top*). EphA-rtk6-AP binding to 95% epiboly (*E*) and six-somite (*F*) embryos is shown, and EphB-rtk8-AP binding to two somite embryos (*G*). The resulting binding patterns look very similar to the expression patterns of *ephrin-A-L1* and *ephrin-B2*, respectively, at comparable stages (Fig. 2C,F,H). Bars, 100 μm.

expression levels of *ephrin-B2* and *ephrin-A-L1* in the paraxial mesoderm, making detection difficult. Protein levels could also be relatively low, leaving little free receptor once it has interacted with its endogenous ligands. It is also possible that endogenous alkaline phosphatase activity, which is particularly difficult to eliminate from within the presomitic mesoderm and somites compared to other regions of the embryo, prevents the detection of low levels of protein in this region.

The results of these AP fusion-binding studies are consistent with the genes already identified, *ephrin-A-L1*, *ephrin-B2*, and *EphA4* being the only members of the Eph family that are expressed in the developing somites, but does not rule out the possible existence of other members with very similar expression profiles.

#### *Interference of Eph family signaling affects somite formation and differentiation*

To study the roles of *EphA4*, *ephrin-A-L1*, and *ephrin-B2* in somitogenesis, truncated and wild-type forms of these genes and of *EphB-rtk8* were overexpressed by injecting capped RNA into one cell of 1- to 4-cell stage zebrafish embryos. Truncated EphA4 (EphA4DN), which lacks the intracellular tyrosine kinase domain, has been used previously to study the role of EphA4 in forebrain and hindbrain development (Xu et al. 1995, 1996). Truncated EphB-rtk8 (EphB-rtk8DN) was constructed in a similar manner. Soluble forms of ephrin-A-L1 (ephrin-A-L1-Tru)

and ephrin-B2 (ephrin-B2-Tru) were also constructed. Another truncated form of ephrin-B2 was also constructed (ephrin-B2-Ic), which has a transmembrane domain but lacks the intracellular domain. This construct should bring about clustering and activation of receptors on binding, but should be incapable of transducing a ligand-dependent signal into the cell expressing the ligand construct.

Overexpression of these constructs predicted to interfere with Eph signaling disrupted somite formation, as did injection of full-length ephrin-B2 (ephrin-B2-WT) (Fig. 4). Control injections of ephrin-B2 or ephrin-A-L1 constructs that lacked the secretion signal sequence or β-galactosidase did not cause any disturbance of somitogenesis. With the injection of any particular species a variety of phenotypes were seen, ranging from the most severe in which somites failed to form, to weaker ones where segmentation produced abnormal shaped somites that were not symmetrical across the midline (Fig. 4A,B). In these weaker cases small extra somites were sometimes seen (Fig. 4D). The number of embryos showing a somite defect, and the severity of this phenotype, depended on the amount of RNA injected. Typically, amounts of RNA were injected that gave 40% embryos showing a weaker phenotype and 7% showing a more severe phenotype for the truncated receptors and soluble ligands; and 60% embryos showing weaker defects and 12% showing more severe ones for ephrin-B2-WT. These variations correspond to the differences in the amount of protein made in vivo from the different constructs (discussed later). It was impossible to distinguish between the phenotypes seen on the injection of the different constructs. It is unclear why both loss of border formation and ectopic boundaries (extra somites) were seen in all cases, as not enough is known of the molecular details and intracellular signaling pathways of Eph receptors and ligands.

Examination of the presomitic mesoderm and somites at the cellular level in injected embryos using the actin stain phalloidin reveals the incorrectly formed somites produced in injected embryos showing a weaker phenotype (Fig. 4D). In normal somites boundaries are symmetrical across the midline and characterized by the presence of columnar epithelial cells on either side of the furrow, whereas cells within the body of the somite are mesenchymal in appearance (Fig. 4C). Five- or six-cell diameters make up the width of the somite along the anteroposterior axis. After the injection of dominant negative constructs of Eph receptors or of soluble ligands the morphology of the somite was disrupted. Where somites formed but were shaped abnormally, the cells at the boundaries showed epithelial morphology. In some cases small groups of cells were seen with the cellular morphology of somites but isolated from the midline by the existence of boundary cells on all sides (Fig. 4D). In experimental embryos defects in intersomitic furrow formation could be seen morphologically at all stages of somitogenesis, and persisted later in development (up to 28 hr postfertilization). The defects in somite morphology did not derive from an increase in cell death as de-



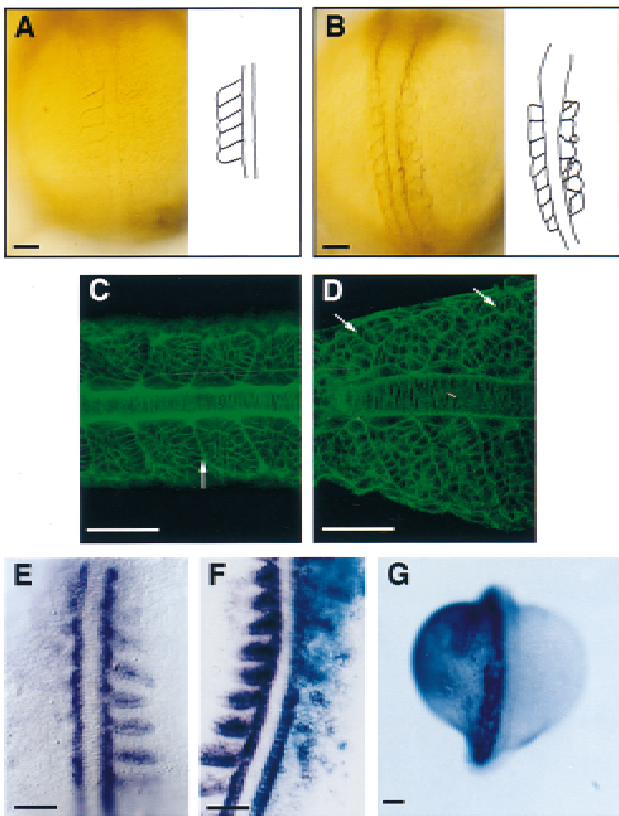


**Figure 4.** Effect of disruption of Eph family signaling on somite formation and differentiation. Embryos were assessed at stages between 4 and 14 somites. Dorsal views, anterior is to the top (except in C and D where anterior is to the left). (A,B) Live embryos injected with ephrin-B2-WT. A camera lucida drawing adjacent to each photo shows the somite boundaries. Somites fail to form (A) or are abnormally shaped and not paired across the midline (B) in affected embryos. (C,D) Confocal microscope images of the somites of phalloidin-stained embryos. (C) A wild-type embryo. The intersomitic furrows (white arrow) and columnar-shaped epithelial cells on either side can be seen. (D) An experimental embryo injected with ephrin-B2-WT. Incorrectly positioned boundaries can be seen in the injected embryos (white arrows), these have columnar-shaped epithelial cells on either side. (E,F) Experimental embryos hybridized to a *myoD* RNA probe (purple). (E) An embryo injected with ephrin-B2-WT; (F) an embryo injected with ephrin-A-L1-Tru. Segmental *myoD* expression is either lost (E) or disrupted (F) on the injected side. The blue color in F is reacted  $\beta$ -galactosidase derived from coinjected RNA. (G) An embryo injected with ephrin-B2-WT reacted with EphB-rtk8-AP to show the presence and localization of ectopic protein. Ectopic ephrin-B2 is found in regions of the somites that are disrupted. Bars, 100  $\mu$ m.

terminated by Nomarski optics, where dying cells have an increased refractive index, (Fig. 4A,B), and TUNEL labeling (data not shown).

Differentiation of somitic cell types as well as boundary formation was affected by disruption of Eph signaling. The commitment of cells to the myogenic lineage is characterized by their expression of the myogenic family of bHLH transcription factors, of which *myoD* is a mem-

ber. The segmental expression of *myoD* was lost in embryos showing the most severe somite phenotypes (Fig. 4E), and was distributed abnormally in embryos showing a weaker phenotype (Fig. 4F). The small somite-like grouping of cells seen by phalloidin staining were also visible in the *myoD* expression pattern suggesting that these small groups of cells behave as somites.

Expression of *myoD* in the adaxial cells was not affected. Adaxial cells are specified by signals from the midline structures before somite formation (Devoto et al. 1996; Blagden et al. 1997), and they are specified normally in zebrafish somite mutants in which boundary formation and segmental *myoD* expression are disturbed (van Eeden et al. 1996). The Eph family does not appear to be required for adaxial cell specification.

#### *Somite defects in the embryo correspond to the localization of protein produced from injected mRNA*

Analysis of protein distribution demonstrated that somite defects were localized to sites of ectopic protein production. The use of the AP fusion proteins gave an indication of the amount and localization of active available protein in the embryos after injection of the various constructs (Fig. 4G). After the injection of RNA at a concentration that results in 30%–40% of embryos showing a somite defect, protein was detected at a concentration of 0.5–0.75 ng bound AP/10 embryos for dominant negative receptors and 1.5–2 ng bound AP/10 embryos for soluble ligands. This is consistent with models of receptor occupancy, where a higher concentration of ligand is required to compete with endogenous protein. A protein level of 0.1–0.2 ng bound AP/10 embryos was obtained after injection of full-length receptor constructs at RNA concentrations that had no effect on somite formation. At higher concentrations of injected RNA severe defects in gastrulation were observed (data not shown). The spatial distribution of the ectopic protein was determined at 70% epiboly, two somites, and ~10 somites. Protein made from the injected RNA species was found in patches in the embryo throughout the period studied. By 10 somites the protein was found on one side of the embryo or in discrete patches. Where protein was detected in the somites, the development of the somites was abnormal (Fig. 4G). Therefore, protein made from injected RNA species was found in the embryo at the stages at which the phenotype described is seen, and in a distribution that corresponds to the site of the defects.

#### *Somite defects can be rescued by coinjecting with full-length receptor*

If somite defects are caused specifically by the interfering versions of Eph receptors or ephrins, then it should be possible to reduce the severity of the defects by competing with wild-type forms of the proteins. Coinjection of RNA encoding either full-length EphA4 or EphB-rtk8 with ephrin-B2-Tru reduced the percentage of defective embryos compared to injection of ephrin-B2-Tru alone (Table 1; Fig. 5A,B). Similarly, coinjection of EphA4 was

**Table 1.** Rescue of somite abnormalities by the coinjection of full-length receptor with truncated ligand

	Full-length receptor			Truncated ligand			Full-length receptor plus truncated ligand		
	no.	S-ab	percent	no.	S-ab	percent	no.	S-ab	percent
EphA4 + <i>ephrin-B2-Tru</i>	84	6	7	90	28	31	111	10	9
EphB-rtk8 + <i>ephrin-B2-Tru</i>	121	7	6	81	23	28	123	14	11
EphA4 + <i>ephrin-A-L1</i>	138	11	8	128	44	34	134	16	12
EphB-rtk8 + <i>ephrin-A-L1</i>	64	5	8	70	18	26	103	27	26

In all cases, RNA encoding  $\beta$ -galactosidase was co-injected. Full-length receptors do not give a somite phenotype (S-ab), whereas the truncated ligands ephrin-B2 and ephrin-A-L1 do. When mixed together and injected the RNAs show different patterns of rescue. The phenotype generated by the truncated form of ephrin-B2 is rescued by both EphA4 and EphB-rtk8, which is consistent with this ligand being able to bind to both of these receptors. In contrast, the phenotype produced by the truncated ephrin-A-L1 is rescued by EphA4 but not by EphB-rtk8, again matching the predictions of the AP fusion ligand and receptor binding studies. (no.) Number of embryos injected; (percent) percentage of injected embryos showing a somite abnormality.

able to rescue the defects caused by injection of ephrin-A-L1-Tru (Table 1). At concentrations effective in rescuing ephrin-B2-Tru-induced defects, EphB-rtk8 was unable to rescue defects caused by ephrin-A-L1-Tru (Table 1; Fig. 5C,D). These results are consistent with the re-

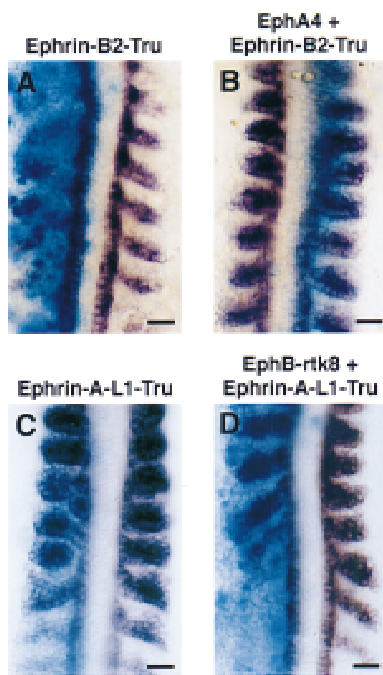


**Figure 5.** Visualization of the rescue experiments using *myoD* expression. Embryos were hybridized with a digoxigenin-labeled antisense RNA *myoD* probe. Embryos are between 10 and 14 somites. Dorsal views, anterior is to the top. Blue staining marks the localization of co-injected  $\beta$ -galactosidase RNA. Embryos shown were injected with (A) ephrin-B2-Tru, (B) EphA4 and ephrin-B2-Tru, (C) ephrin-A-L1-Tru, and (D) EphB-rtk8 and ephrin-A-L1-Tru. Disrupted segmental *myoD* expression is seen on the injection of truncated forms of ephrin-B2 (A) and ephrin-A-L1 (C). Coinjection of EphA4 with ephrin-B2-Tru rescues the *myoD* expression (B); whereas coinjection of EphB-rtk8 has no effect on the ephrin-A-L1-Tru phenotype (D). Bars, 50  $\mu$ m.

ceptor-binding profiles determined in vitro and indicate that the somite phenotypes seen in embryos injected with ephrin-A-L1-Tru and ephrin-B2-Tru are attributable to disruption of endogenous Eph family signaling. To ensure that when two species of RNA were injected both were translated we determined the protein levels of ephrin-A-L1-tru and EphB-rtk8 in embryos that had been injected with RNA encoding these two proteins in isolation or when coinjected. The protein levels determined were 0.28 and 0.30 ng bound AP/10 embryos for ephrin-A-L1-Tru and 0.50 and 0.63 ng bound AP/10 embryos for EphB-rtk8 in isolation and when coinjected, respectively. This suggests that rescue by coinjection of two different RNA species, at these concentrations, does not result from an overloading of the translation machinery and a reduction in the level of active protein. Therefore, the observed defects in somitogenesis are a specific result of interfering with Eph family signaling.

#### *Eph family signaling is required for the regulation of her1, Delta D, and paraxis expression in the presomitic mesoderm*

To determine whether the somite defects derived from the effects of exogenous Eph proteins during gastrulation, in situ hybridizations with probes to *no tail (ntl)*, *snail1 (sna1)*, and *her1* were carried out on injected embryos between the stages of 60% and 90% epiboly. *Ntl* and *sna1* are expressed in the germ ring and involuting mesoderm during gastrulation (Schulte-Merker et al. 1994; Thisse et al. 1994) and, therefore, are good indicators of the normal progress of gastrulation. The expression patterns of these two genes and of *her1* were normal during these stages (data not shown), indicating that gastrulation was not disrupted in injected embryos and that mesoderm migration was unaffected.

During the late stages of gastrulation, 75%–100% epiboly, *her1* is restricted to a segmental prepatter. This was also seen in injected embryos showing that the segmental prepatter is laid down correctly in injected embryos. However, from bud stage *her1* expression was disturbed in injected embryos, the anterior stripe of ex-

pression was regulated consistently abnormally in experimental embryos (Fig. 6B,C).

The expression patterns of genes known to be involved in somite formation, *her1*, *Delta D*, and *paraxis (par1)*, and patterning, *FGF-8*, were examined in injected embryos at the 8- to 12-somite stage when defects in boundary formation were clearly visible. The analysis of all markers was carried out for embryos in which the ephrins ephrin-B2-WT, ephrin-B2-Tru, ephrin-B2-Ic, or ephrin-A-L1-Tru and the receptors EphB-rtk8DN or EphA-4DN had been overexpressed. The results were essentially the same for each of these cases and representative

embryos are shown in Figure 6. The severity and number of embryos affected varied between different injection experiments depending on the amount of RNA injected and ectopic protein produced in vivo. The disruptions seen in the expression of the marker genes reflected the number and degree of morphological defects observed within each experimental batch of embryos.

At the 8- to 12-somite stage in control embryos *her1* is expressed in two or three stripes in the presomitic mesoderm that correspond to the primordia of alternating odd numbered somites (Fig. 6D; Muller et al. 1996). The effects of RNA injections on *her1* expression varied; in

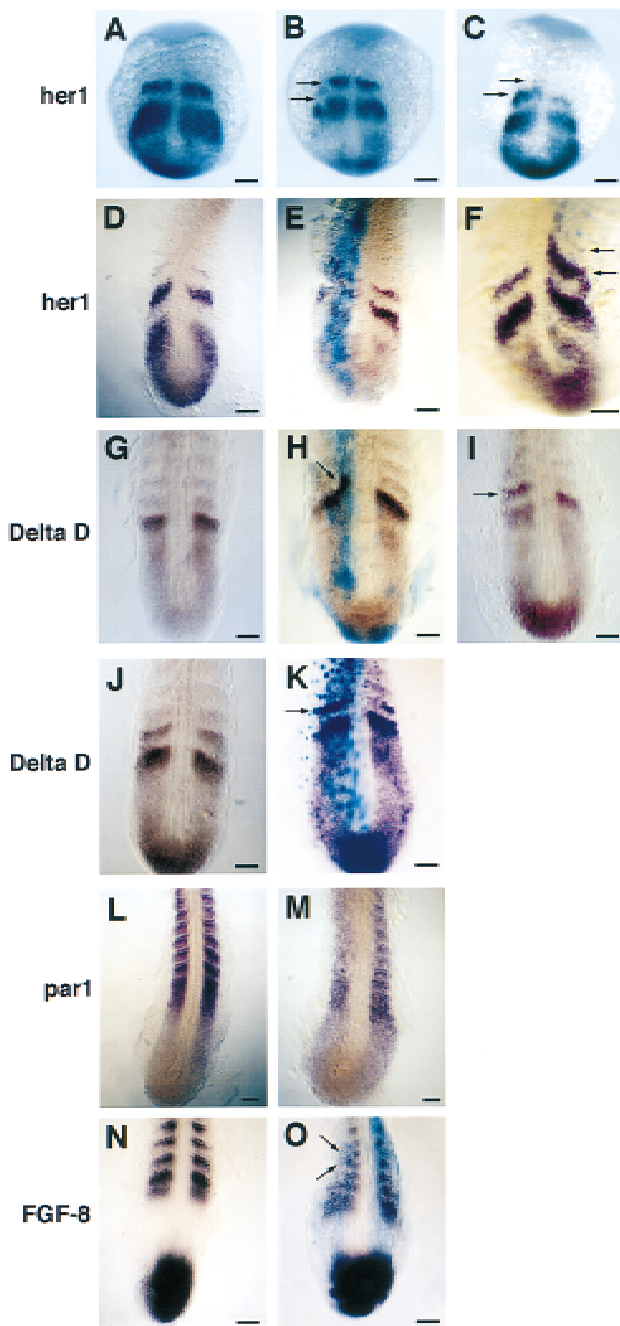


**Figure 6.** Effect of the disruption of Eph family signaling on the segmental pattern in the presomitic mesoderm and on patterning of the somites. Dorsal views, anterior is to the top. Blue staining (E,F,H,K,O) marks localization of coinjected  $\beta$ -galactosidase RNA. (A) Wild-type *her1* expression in a two-somite embryo. (B,C) *her1* expression in two-somite embryos injected with ephrin-B2-WT. The anterior stripes of *her1* expression are either disrupted (arrows in B), or expression is maintained anteriorly such that extra stripes are seen (arrows in C), on the injected side. (D) Wild-type expression of *her1* in a 12-somite embryo. (E,F) *her1* expression in 12-somite embryos injected with ephrin-B2-WT and EphB-rtk8DN, respectively. Once again the anterior stripes of *her1* expression are either disturbed (injected side in E), or expression is not switched off correctly, resulting in the presence of an extra stripe anteriorly (arrows in F). (G,J) The dynamic nature of *Delta D* expression in 12-somite control embryos, either one (G) or two (J) stripes are seen in the anterior presomitic mesoderm. (H,I,K) *Delta D* expression in embryos injected with ephrin-B2-WT, ephrin-B2-Ic, and EphB-rtk8DN, respectively. *Delta D* expression is incorrectly regulated in injected embryos, resulting in disrupted stripes (arrow in H), or persistence of expression such that extra stripes are seen anteriorly on the injected side (arrows in I and K). (L) Wild-type expression of *par1* in a 12-somite embryo. (M) *par1* expression in a 12-somite embryo injected with ephrin-B2-WT. *Par1* is not restricted to its usual segmental pattern on the injected side where somites have failed to form. (N) Wild-type *FGF-8* expression in a 12-somite embryo. (O) *FGF-8* expression in a 12-somite embryo injected with ephrin-B2-Ic. *FGF-8* is expressed in an anterior domain of abnormally shaped somites in the injected embryo (arrows in O). (A-C) Bar, 50  $\mu$ m; (D-O) bar, 100  $\mu$ m.



some cases irregularly shaped stripes or small patches of *her1* expression were found (Fig. 6E), and in others the expression was disrupted and shifted anteriorly by the distance of approximately one band of *her1* expression (Fig. 6F). However, expression of *her1* was maintained caudally in the tail bud. Somites failed to form in embryos with an extra band of *her1* expression.

In control 8- to 12-somite embryos zebrafish *Delta D* is expressed at high levels in one or two stripes in the anterior presomitic mesoderm, at a lower level in the anterior of each of the formed somites and in the extending tailbud (Fig. 6G,J; Dornseifer et al. 1997). In experimental embryos expression of *Delta D* was disrupted and shifted anteriorly in regions where somite formation had been disturbed but was not affected in the tailbud (Fig. 6H,I,K). In embryos that failed to segment an extra stripe of *Delta D* expression was seen anterior to its normal expression domain on the injected side (Fig. 6I,K).

A zebrafish *paraxis* gene, *par1*, has been cloned recently (Shanmugalingam and Wilson 1998). In control embryos *par1* expression is detected uniformly throughout the presomitic mesoderm but after somite formation it is stronger in an anterior domain of each somite (Fig. 6L). This expression pattern is similar to that described for the mouse homolog (Burgess et al. 1995). Injected embryos showing a somite phenotype also had a disrupted *par1* expression pattern; in regions where somites failed to form *par1* expression was not restricted to its usual segmental pattern, but remained expressed uniformly, as in the presomitic mesoderm (Fig. 6M).

These results suggest that Eph signaling is not required for the establishment of the segmental prepatterning in the paraxial mesoderm. However, disruption of Eph signaling does affect the regulation and switching off of both *her1* and *Delta D* in the anterior presomitic mesoderm, as well as the regulation of *par1* gene expression.

As an indication of anteroposterior patterning within the disrupted somites in situ hybridization with probes for *FGF-8* or *myoD* as performed. At the 10-somite stage *FGF-8* is expressed throughout the anterior presomitic mesoderm and becomes restricted to an anterior domain of cells in the formed somites (Fig. 6N). In injected embryos *FGF-8* expression was restricted to an anterior domain even within the abnormally shaped somites (Fig. 6O). Also in the affected somites *myoD* expression was detected in a posterior domain as is the case in normally formed somites at these stages (see Fig. 4F). These results indicate that the anteroposterior patterning within the somites is not affected by disruption of Eph signaling.

#### Relationship between EphA4, ephrin-B2, and *her1* expression

Because the timing of the defects in *her1* expression corresponded to the onset of segmental expression of *EphA4* and *ephrin-B2* in the presomitic mesoderm, we investigated in more detail, the relationship between *her1* expression and these genes. Double in situ hybridizations with probes for *EphA4* plus *ephrin-B2*, *her1* plus *EphA4*,

and *her1* plus *ephrin-B2* were undertaken in control embryos (Fig. 7).

*ephrin-B2* and *EphA4* are expressed in alternating stripes in the somites and presomitic mesoderm with *EphA4* being in the anterior cells of each somite and *ephrin-B2* in the posterior cells (Fig. 7A). There is an interface between these expression domains within each somite and within the most anterior presumptive

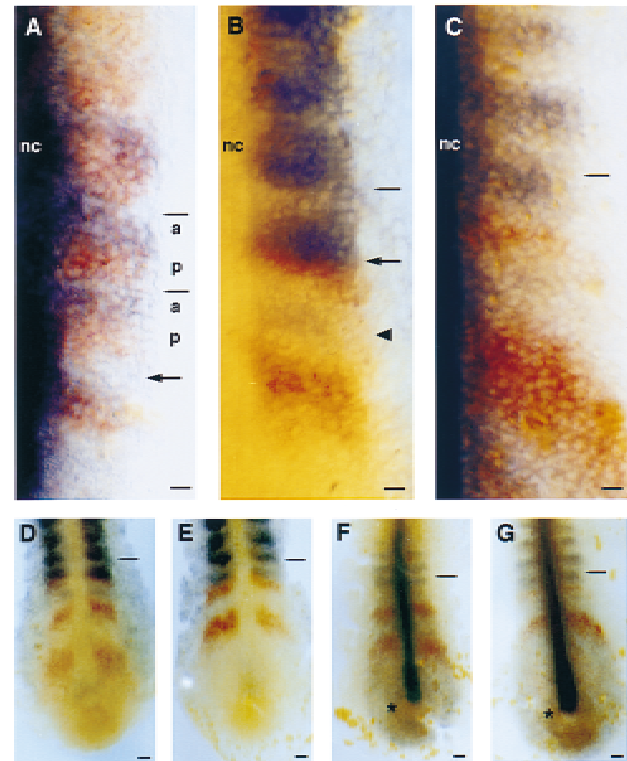


**Figure 7.** Relationship of *ephrin-B2*, *EphA4*, and *her-1* expression in the anterior presomitic mesoderm and posterior somites. Embryos were hybridized with digoxigenin- and fluorescein-labeled antisense RNA probes. Dorsal views, anterior is to the top, of six-somite (A,B,C,D,E,G) and five-somite (F) stage embryos. (A) *EphA4* (blue) is expressed in an anterior domain of the formed somites and most anterior presumptive somites, whereas *ephrin-B2* (red) is expressed in a posterior domain of these segments (lines mark the two most posterior somite boundaries). In the anterior presomitic mesoderm a row of non-expressing cells is found at the position where the next somite boundary will form (arrow). (B,D,E) *ephrin-B2* (blue) and *her-1* (red) expression. *Her1* expression is lost in an anterior to posterior direction in the most anterior presumptive somite (line marks the last formed somite boundary), which corresponds with the posterior expansion of the *ephrin-B2* expression domain in the same region, such that cells expressing both genes are seen (arrow in B). Expression of *ephrin-B2* is seen between the two most anterior stripes of *her1* expression (arrowhead in B). (C,F,G) *EphA4* (blue) and *her-1* (red) expression. *EphA4* and *her1* expression are not seen juxtaposed in the anterior presomitic mesoderm (line marks the last formed somite boundary). Low level expression of *EphA4* is also seen throughout the paraxial mesoderm (stars in F and G). (a) Anterior; (nc) notochord; (p) posterior; bars, 50  $\mu$ m.

somites. *EphA4* and *ephrin-B2* expression domains also meet where boundaries have formed. However, within the presomitic mesoderm, at the position where the next somite boundary is to form, there is a single row of non-expressing cells between the *ephrin-B2* and *EphA4* expression domains. *ephrin-B2* expression expands caudally such that once a somite has formed there is no longer a gap between the expression of these two genes.

*Her1* is expressed in bands of cells of one somite width in the presomitic mesoderm alternating with regions of similar width devoid of *her1* expression. These bands of expression correspond to somitic primordia (Muller et al. 1996). As the presumptive somite develops, *her1* expression is lost in an anterior to posterior direction (Muller et al. 1996; Fig. 7). The expression and subsequent caudal expansion of *ephrin-B2* within the presomitic mesoderm corresponds to the timing of the reduction in *her1* expression within its most anterior domain and cells coexpressing both genes are seen (Fig. 7B,D,E). *EphA4* is expressed in the anterior of the formed and the most anterior-forming somites. The distance between the *EphA4* and *her1* expression domains varied significantly as a result of *her1* being expressed only in alternate somite primordia (Fig. 7C,F,G).

## Discussion

The results presented here demonstrate a role for Eph signaling in the formation and differentiation of somites. We demonstrate the iterative expression of members of this family within the presomitic and somitic mesoderm and illustrate that interfering with Eph signaling leads to loss or incorrect formation of somite boundaries and disruption of myogenic differentiation. The defects in boundary formation are reminiscent of those reported on disturbance of Notch/Delta signaling (Conlon et al. 1995; Dornseifer et al. 1997; Jen et al. 1997) and disruption of Eph signaling prevents the correct regulation of *Delta D* expression in the developing somites. These results suggest that Notch/Delta signaling and Eph signaling may function together to establish somite boundaries. We have investigated the mechanism underlying the somite defect with regard to the segmental pattern as illustrated by *her1* expression. The results show that the establishment of this segmental pattern is unaffected by disruption of Eph signaling, rather it is the translation of the prepattern into somites that is disturbed.

### *Eph signaling affects the translation of the segmental prepattern into somites*

Evidence for the existence of a segmental pattern within the presomitic mesoderm came from embryological experiments including transplantation of presomitic tissue in chicks and heat shock of *Xenopus* embryos (Keynes and Stern 1988; Gossler and Hrabe de Angelis 1998). These results suggest that the process of segmentation is organized in the presomitic mesoderm before the somite boundaries are formed. Recently molecular evidence for

the existence of this presomitic segmental pattern has been obtained. Homologs of the *Drosophila* pair-rule gene *hairy*, which is involved in embryonic segmentation, have been cloned in zebrafish, *her1*, and chick, *c-hairy-1*. *her1* is expressed in stripes in the presomitic mesoderm that correspond to alternate somite primordia (Muller et al. 1996), whereas *c-hairy-1* has a dynamic expression pattern that passes through a characteristic cycle during the formation of each somite (Palmeirim et al. 1997). How the segmental pattern is established in the presomitic mesoderm remains unclear, although the *c-hairy-1* expression pattern provides molecular evidence for the existence of a developmental clock linked to segmentation (Cooke 1998). This is consistent with the Clock and Wavefront model (Cooke and Zeeman 1976), which proposes that a segmental pattern is established through the interaction of two components that are temporally and spatially regulated. The disruption of Eph family signaling does not affect the establishment of the prepattern, indicating that Eph function is not required for this process. However, the later regulation of *her1* expression is disrupted and subsequently, somites fail to form or form aberrantly. This suggests that Eph family signaling is required to translate the prepattern into the events of somite boundary formation and differentiation (Fig. 8). These processes appear to require the switching off of transcriptional repressors such as *her1*, and the refinement of expression patterns of signaling molecules such as *Delta D*.

### *Anteroposterior polarity exists within the presumptive somites*

The expression patterns of *ephrin-B2* and *EphA4* within the anterior presomitic mesoderm indicate that the presumptive somites are patterned along the anteroposterior axis before boundary formation, as *ephrin-B2* is expressed within a posterior domain and *EphA4* an anterior domain of the most rostral somite primordia. In addition, the signaling proteins Delta D and FGF-8 also become restricted to the anterior domain of the somite as segmentation occurs (Dornseifer et al. 1997; Furthauer et al. 1997; Fig. 6J,N). In contrast, *myoD* is expressed in the posterior part of the somite from the 10-somite stage (Weinberg et al. 1996). These anteroposterior restrictions of Eph, FGF, and Delta signaling proteins before, or as segmentation occurs, suggest that anteroposterior patterning of each segment is occurring in the presomitic mesoderm. The existence of an anteroposterior pattern within presumptive somites was also suggested by grafting experiments in chicks, in which a boundary was only seen to form when anterior and posterior somite cells were juxtaposed (Stern and Keynes 1987).

### *Expression of EphA4 and ephrin-B2 suggest a role in boundary formation*

In *Xenopus*, chick, rat, and mouse a number of members of the Eph family are expressed in the somites, including *EphA3*, *EphB3*, *ephrin-B1*, and *ephrin-A5* (Fletcher et al.

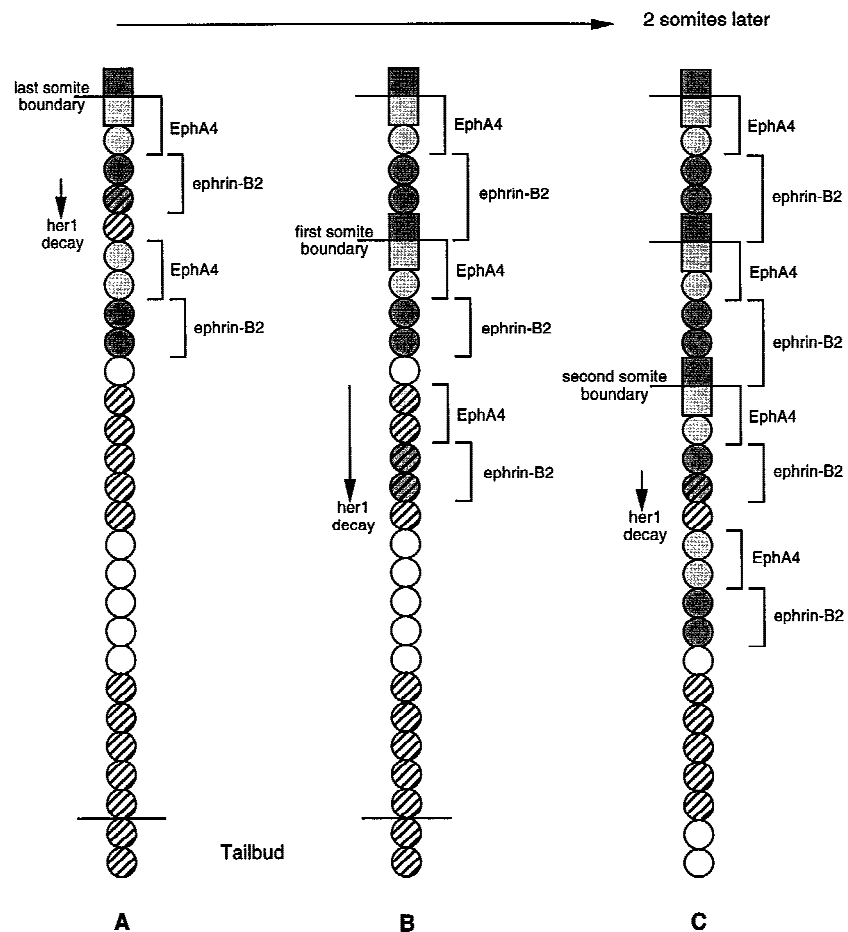


**Figure 8.** Diagrammatic representation of the relationship between *her1*, *EphA4*, and *ephrin-B2* in a single file of cells along the anteroposterior axis of the paraxial mesoderm during somitogenesis. The three columns represent the cells over a period of time during which two somites are added. *her1* expression is shown in hatched circles, *EphA4* expression in light shading, and *ephrin-B2* expression in dark shading. Where *her1* and *EphA4* expression overlap lightly shaded hatched circles are used, and where *her1* and *ephrin-B2* expression overlap darkly shaded hatched circles are used.

1994; Kilpatrick et al. 1996). Only *EphA4* and *ephrin-B2* have been shown previously to be expressed segmentally in the presomitic mesoderm in mouse and chick (Bergemann et al. 1995; Irving et al. 1996). In zebrafish *EphA4* and *ephrin-B2* are expressed sequentially along the anteroposterior axis of the embryo within the somitic and anterior presomitic mesoderm. The similarity of the expression patterns of these two genes in zebrafish and higher vertebrates suggest that their function within the presomitic mesoderm may be conserved. In zebrafish somites form by a process of local deadhesion within the presomitic mesoderm (Wood and Thorogood 1994). As the Eph family of proteins have been shown to mediate an inhibition of cell movement and growth cone collapse (Drescher et al. 1995; Brennan et al. 1997; Wang and Anderson 1997), and the temporal and spatial expression patterns of *EphA4* and *ephrin-B2* correlate with boundary formation, these are suitable molecules to play a role in this process of deadhesion. These proteins also play a role in segmentation in the hindbrain (Xu et al. 1995).

In zebrafish, as a somite boundary forms the cells on either side of the border undergo a shape change from mesenchymal to epithelial (Fig. 4C,D). As class B ephrins have been shown to be capable of intracellular signaling, the presence of *ephrin-B2* in cells on one side of the boundary and *EphA4* in cells on the other suggests that

bidirectional signaling by way of these molecules could be involved in the cell shape changes required for furrow formation. The Eph family of receptors have been shown to associate with the GTPase rasGAP (Holland et al. 1997) and the SH2 domain containing adapter protein Nck (Stein et al. 1998), both of which are able to influence cytoskeletal architecture (McGlade et al. 1993). Also, alterations of both the actin cytoskeleton and microtubules have been visualized in axon growth cones after their exposure to A and B class ephrins (Meima et al. 1997a,b). These observations show that Eph receptors are capable of affecting the cytoskeleton, and therefore could mediate the cell shape changes required for somite boundary formation. Juxtaposition of *EphA4* and *ephrin-B2*-expressing cells is not the only requirement for boundary formation, as these are also expressed in adjacent cells in the center of each somite where no boundary forms. This suggests that Eph signaling acts coordinately with other processes to bring about somite boundary formation.

## Materials and methods

### Maintenance of fish

Breeding fish were maintained at 28.5°C on a 14-hr light/10-hr

dark cycle. Embryos were collected by natural spawning and staged according to Kimmel et al. (1995).

#### *cDNA cloning and sequencing*

*Ephrin-A-L1* was cloned as previously described (Brennan et al. 1997). For the cloning of *ephrin-B2* degenerate primers were designed to conserved regions (FTIKFQE and YYIVQEM) and were used for amplification of a zebrafish neurula stage library. The PCR product was used as a probe to screen the neurula stage cDNA library at low stringency. Individual clones containing the entire open reading frame of *ephrin-B2* were isolated (GenBank accession no. AJ004863).

Partial cDNA clones encoding the 5' region of the Eph class B receptor *EphB-rtk8* coding sequence were isolated after high stringency screening of a random primed 3- to 15-hr zebrafish cDNA library. A 0.2-kb fragment of a previously isolated partial cDNA of *EphB-rtk8* (Cooke et al. 1997) was used as the probe. The entire open reading frame of *EphB-rtk8* was then contained within two overlapping cDNA clones (GenBank accession no. AJ005029).

#### *Cytoskeleton staining*

Phalloidin staining was performed as described previously (Whitfield et al. 1996).

#### *Detection of cell death*

Cell death was detected by the method of terminal transferase dUTP nick end labeling (TUNEL, ApopTag In situ Apoptosis Detection Kit, Peroxidase; Oncor Inc.) (Abdelilah et al. 1996).

#### *Whole mount in situ hybridization and immunostaining*

Whole mount in situ hybridization using digoxigenin-labeled anti-sense RNA probes was performed as described (Xu et al. 1994).

#### *Whole mount and cell alkaline phosphatase binding studies*

Whole mount alkaline phosphatase-binding studies were performed as described previously (Cheng and Flanagan 1994; Brennan et al. 1997).

#### *Quantitative assay for APTag-Eph protein binding to embryos*

To quantitate the amount of ectopic protein made after the injection of RNA encoding Eph family proteins we determined the amount of AP fusion protein bound to the embryos using the colorimetric method of Berger et al. (1988; Flanagan and Leder 1990).

#### *Preparation of synthetic RNA and microinjection of zebrafish embryos*

Capped RNA was synthesized by in vitro transcription of linearized plasmids and RNA concentration was determined spectrophotometrically. RNA was injected in a volume of ~200  $\mu$ l into one cell of a one- to four-cell stage zebrafish embryo, using a glass capillary needle attached to a Picospritzer. The amount of RNA injected was, for the ligand constructs 60–100 ng/ $\mu$ l, and for the dominant negative receptor constructs 300–400 ng/ $\mu$ l and 150–200ng/ $\mu$ l for the full-length receptor constructs.

To control for nonspecific effects of RNA injection, ephrin-A-L1 and ephrin-B2 constructs that lack signal sequences were

injected. The distribution of injected RNA in vivo was determined by coinjecting with RNA encoding  $\beta$ -galactosidase. The two species of RNA broadly segregate together during development (Griffin et al. 1995), and the distribution of  $\beta$ -galactosidase can be determined subsequently by staining for enzyme activity.

#### **Acknowledgments**

We thank our colleagues in the Holder and Wilson laboratories for their comments and criticisms during the course of this work. We thank Leila Abbas and Juliet Williams for help with phalloidin and TUNEL staining, respectively. We also thank Jose Campos-Ortega, Eric Weinberg, David Wilkinson, John Flanagan, Julian Lewis, and Didier Stainier for providing us with probes. Thanks also to Steve Wilson, Simon Hughes, Rudiger Klein, Andrew Boyd, and Martin Lackmann for discussions and for sharing their results before publication. The work was supported financially by the Wellcome Trust, a Biotechnology and Biological Sciences Council Research (BBSRC) program grant, the Medical Research Council, and the Human Frontier Science Program. K.S. is a recipient of a Japanese Society for the Promotion of Science postdoctoral fellowship for research abroad.

The publication costs of this article were defrayed in part by payment of page charges. This article must therefore be hereby marked 'advertisement' in accordance with 18 USC section 1734 solely to indicate this fact.

#### **References**

- Abdelilah, S., E. Mountcastle-Shah, M. Harvey, L. Solnica-Krezel, A. Schier, D. Stemple, J. Malicki, S. Neuhauss, F. Zwartkruis, D. Stainier, Z. Rangini, and W. Driever. 1996. Mutations affecting neural survival in the zebrafish *Danio rerio*. *Development* **123**: 217–227.
- Bartley, T. D., R.W. Hunt, A.A. Welcher, W.J. Boyle, V.P. Parker, R.A. Lindberg, H.S. Lu, A.M. Colombero, R.A. Elliot, B.A. Guthrie, P.L. Holst, J.D. Skrine, R.J. Toso, M. Zhang, E. Fernandez, G. Trail, T. Hunter, and G.M. Fox. 1994. B61 is a ligand for the ECK receptor protein-tyrosine kinase. *Nature* **368**: 558–560.
- Bergemann, A., C. Hwai-Jong, R. Brambilla, R. Klein, and J. Flanagan. 1995. Elf-2, a new member of the Eph ligand family, is segmentally expressed in mouse embryos in the region of the hindbrain and newly forming somites. *Mol. Cell. Biol.* **15**: 4921–4929.
- Berger, J., J. Hauber, R. Hauber, R. Geiger, and B. Cullen. 1988. Secreted placental alkaline phosphatases: A powerful new quantitative indicator of gene expression in eukaryotic cells. *Gene* **66**: 1–10.
- Blagden, C., P. Currie, P. Ingham, and S. Hughes. 1997. Notochord induction of zebrafish slow muscle is mediated by sonic hedgehog. *Genes & Dev.* **11**: 2163–2175.
- Brambilla, R., A. Schnapp, F. Casagrande, J. Labrador, A. Bergemann, J. Flanagan, E. Pasquale, and R. Klein. 1995. Membrane bound LERK2 ligand can signal through three different Eph-related receptor tyrosine kinases. *EMBO J.* **14**: 3116–3126.
- Brennan, C., B. Monshau, R. Lindberg, B. Guthrie, U. Drescher, F. Bonhoeffer, and N. Holder. 1997. Two Eph receptor tyrosine kinase ligands control axon growth and may be involved in the creation of the retinotectal map in zebrafish. *Development* **124**: 655–664.
- Bruckner, K., E. Pasquale, and R. Klein. 1997. Tyrosine phosphorylation of transmembrane ligands for Eph receptors. *Sci-*



- ence* **275**: 1640–1643.
- Burgess, R., P. Cserjesi, K. Ligon, and E. Olson. 1995. Paraxis: A basic helix-loop-helix protein expressed in paraxial mesoderm and developing somites. *Dev. Biol.* **168**: 296–306.
- Cheng, H.-J. and J. Flanagan. 1994. Identification and cloning of ELF-1, a developmentally expressed ligand for the Mek4 and Sek1 receptor tyrosine kinases. *Cell* **79**: 157–168.
- Conlon, R., A. Reaune, and J. Rossant. 1995. Notch1 is required for the coordinate segmentation of somites. *Development* **121**: 1533–1545.
- Cooke, J. 1998. A gene that resuscitates a theory—Somitogenesis and a molecular oscillator. *Trends Genet.* **14**: 85–88.
- Cooke, J. and E. Zeeman. 1976. A clock and wavefront model for control of the numbers of repeated structures during animal morphogenesis. *J. Theoret. Biol.* **58**: 455–476.
- Cooke, J., Q. Xu, S. Wilson, and N. Holder. 1997. Characterisation of five novel zebrafish Eph-related receptor tyrosine kinases suggests roles in neural patterning. *Genes Dev. Evol.* **206**: 515–531.
- Devoto, S., E. Melancon, J. Eisen, and M. Westerfield. 1996. Identification of separate slow and fast muscle precursor cells in vivo, prior to somite formation. *Development* **122**: 3371–3380.
- Dornseifer, P., C. Takke, and J. Campos-Ortega. 1997. Overexpression of a zebrafish homologue of the Drosophila neurogenic gene Delta perturbs differentiation of primary neurons and somite development. *Mech. Dev.* 1–13.
- Drescher, U., C. Kremoser, C. Handwerker, J. Loschinger, M. Noda, and F. Bonhoeffer. 1995. In vitro guidance of retinal ganglion cell axons by RAGS, a 25kDa tectal protein related to the ligands for Eph receptor tyrosine kinases. *Cell* **82**: 359–370.
- Flanagan, J. and P. Leder. 1990. The Kit ligand: A cell surface molecule altered in steel mutant fibroblasts. *Cell* **63**: 185–194.
- Flenniken, A., N. Gale, G. Yancopoulos, and D. Wilkinson. 1996. Distinct and overlapping expression patterns of ligands for Eph related receptor tyrosine kinases during mouse development. *Dev. Biol.* **179**: 382–401.
- Fletcher, F., M. Carpenter, H. Shilling, P. Baum, S. Ziegler, S. Gimpel, T. Hollingsworth, T. Vanden Bos, L. James, K. Hjerrild, B. Davison, S. Lyman, and M. Beckmann. 1994. LERK-2, a binding protein for the receptor-tyrosine kinase ELK, is evolutionarily conserved and expressed in a developmentally regulated pattern. *Oncogene* **9**: 3241–3247.
- Furthaver, M., C. Thisse, and B. Thisse. 1997. A role for FGF-8 in the dorsoventral patterning of the zebrafish gastrula. *Development* **124**: 4253–4264.
- Gale, N. and G. Yancopoulos. 1997. Ephrins and their receptors: A repulsive topic. *Cell Tiss. Res.* **290**: 227–241.
- Gale, N., S. Holland, D. Valenzuela, A. Flenniken, L. Pan, T. Ryan, M. Henkemeyer, K. Strebhardt, H. Hirai, D. Wilkinson, T. Pawson, S. Davis, and G. Yancopoulos. 1996. Eph receptors and ligands comprise two major specificity subclasses and are reciprocally compartmentalized during embryogenesis. *Neuron* **17**: 9–19.
- Gossler, A. and M. Hrabe de Angelis. 1998. Somitogenesis. *Curr. Top. Dev. Biol.* **38**: 225–287.
- Griffin, K., R. Patient, and N. Holder. 1995. Analysis of FGF function in normal and no tail zebrafish embryos reveals separate mechanisms for formation of the trunk and tail. *Development* **121**: 2983–2994.
- Holland, S., N. Gale, G. Gish, R. Roth, Z. Songyang, L. Cantley, M. Henkemeyer, G. Yancopoulos, and T. Pawson. 1997. Juxtamembrane tyrosine residues couple the Eph family receptor EphB2/Nuk to specific SH2 domain proteins in neuronal cells. *EMBO J.* **16**: 3877–3888.
- Holland, S., N. Gale, G. Mbamalu, G. Yancopoulos, M. Henkemeyer, and T. Pawson. 1996. Bidirectional signaling through the Eph-family receptor Nuk and its transmembrane ligands. *Nature* **383**: 722–725.
- Irving, C., A. Nieto, R. DasGupta, P. Charnay, and D. Wilkinson. 1996. Progressive spatial restriction of Sek-1 and krox-20 gene expression during hindbrain segmentation. *Dev. Biol.* **173**: 26–38.
- Jen, W., D. Wettstein, D. Turner, A. Chitnis, and C. Kintner. 1997. The Notch ligand, X-Delta-2, mediates segmentation of the paraxial mesoderm in *Xenopus* embryos. *Development* **124**: 1169–1178.
- Keynes, R. and C. Stern. 1988. Mechanisms of vertebrate segmentation. *Development* **103**: 413–429.
- Kimmel, C.B., W.W. Ballard, S.R. Kimmel, B. Ullmann, and T. F. Schilling. 1995. Stages of embryonic development of the zebrafish. *Devel. Dyn.* **203**: 253–310.
- Kilpatrick, T., A. Brown, C. Lai, M. Gassman, M. Goulding, and G. Lemke. 1996. Expression of the Tyro4/Mek4/Cek4 gene specifically marks a subset of embryonic motor neurons and their muscle targets. *Mol. Cell. Neurosci.* **7**: 62–74.
- Krull, C., R. Lansford, N. Gale, A. Collazo, C. Marcelle, G. Yancopoulos, S. Fraser, and M. Bronner-Fraser. 1997. Interactions of Eph-related receptors and ligands confer rostrocaudal pattern to trunk neural crest migration. *Curr. Biol.* **7**: 571–580.
- McGlade, J., B. Brunkhorst, D. Anderson, G. Mbamalu, J. Settlementman, S. Dedhar, M. Rozakis-Adcock, L. Bo Chen, and T. Pawson. 1993. The N-terminal region of GAP regulates cytoskeletal structure and cell adhesion. *EMBO J.* **12**: 3073–3081.
- Macdonald, R., J. Scholes, U. Strahle, C. Brennan, N. Holder, M. Brend, and S. Wilson. 1997. The Pax protein Noi is required for commissural axon pathway formation in the rostral forebrain. *Development* **124**: 2397–2408.
- Meima, L., I. Kljavin, P. Moran, A. Shih, J. Winslow, and I. Carras. 1997a. AL-1 induced growth cone collapse of rat cortical neurons is correlated with REK-7 expression and rearrangement of the actin cytoskeleton. *Eur. J. Neurosci.* **9**: 177–188.
- Meima, L., P. Moran, W. Mathews, and I. Caras. 1997b. Lerk2 (ephrin-B1) is a collapsing factor of a subset of cortical growth cones and acts by a mechanism different from AL-1 (ephrin-A5). *Mol. Cell. Neurosci.* **9**: 314–328.
- Muller, M., E. Weizsacker, and J. Campos-Ortega. 1996. Expression domains of a zebrafish homologue of the Drosophila pair-rule gene hairy correspond to a primordia of alternating somites. *Development* **122**: 2071–2078.
- Palmeirim, I., D. Henrique, D. Ish-Horowicz, and O. Pourquie. 1997. Avian hairy gene expression identifies a molecular clock linked to vertebrate segmentation and somitogenesis. *Cell* **28**: 639–648.
- Saga, Y., N. Hata, H. Koseki, and M. Taketo. 1997. *Mesp2*: A novel mouse gene expressed in the presegmented mesoderm and essential for segmentation initiation. *Genes & Dev.* **11**: 1827–1839.
- Scales, J., R. Winning, C. Renaud, L. Shea, and T. Sargent. 1995. Novel members of the eph receptor kinase subfamily expressed during *Xenopus* development. *Oncogene* **11**: 1745–1752.
- Schulte-Merker, S., F. Van Eeden, M.E. Halpern, C.B. Kimmel, and C. Nüsslein-Volhard. 1994. *no tail (ntl)* is the zebrafish homolog of the mouse *T (Brachyury)* gene. *Development* **124**: 1009–1015.
- Shanmugalingam, S. and S. Wilson. 1998. Isolation, expression

- and regulation of a zebrafish *paraxis* homologue. *Mech. Dev.* (in press).
- Smith, A., V. Robinson, K. Patel, and D. Wilkinson. 1997. The EphA4 and EphB1 receptor tyrosine kinases and ephrin-B2 ligand regulate targeted migration of branchial neural crest cells. *Curr. Biol.* **7**: 561–570.
- Stein, E., U. Huynh-Do, A. Lane, D. Cerreti, and T. Daniel. 1998. Nck recruitment to Eph receptor, EphB1/ELK, couples ligand activation to c-Jun kinase. *J. Biol. Chem.* **272**: 1303–1308.
- Stern, C. and R. Keynes. 1987. Interactions between somite cells: The formation and maintenance of segment boundaries in the chick embryo. *Development* **99**: 261–272.
- Taneja, R., B. Thisse, F. Rijli, C. Thisse, P. Bouillet, P. Dolle, and P. Chambon. 1996. The expression pattern of the mouse receptor tyrosine kinase gene MDK1 is conserved through evolution and requires Hoxa-2 for rhombomere-specific expression in mouse embryos. *Devel. Dyn.* **177**: 397–412.
- Thisse, C., B. Thisse, T. Schilling, and J. Postlethwaite. 1994. Structure of the zebrafish *snail1* gene and its expression in wildtype, spadetail and notail mutant embryos. *Development* **119**: 1203–1215.
- van Eeden, F., M. Granato, U. Schach, M. Brand, M. Furutani-Seiki, P. Haffter, M. Hammerschmidt, C.-P. Heisenberg, Y.-J. Jiang, D. Kane, R. Kelsh, M. Mullins, J. Odenthal, R. Warga, M. Allende, E. Weinberg, and C. Nüsslein-Volhard. 1996. Mutations affecting somite formation and patterning in the zebrafish, *Danio rerio*. *Development* **123**: 153–164.
- Wang, H. and D. Anderson. 1997. Eph family transmembrane ligands can mediate repulsive guidance of trunk neural crest migration and motor axon outgrowth. *Neuron* **18**: 383–396.
- Weinberg, E., M. Allende, C. Kelly, A. Abdelhamid, P. Andermann, G. Doerre, D. Grunwald, and B. Riggelman. 1996. Developmental regulation of zebrafish MyoD in wildtype, no tail and spadetail embryos. *Development* **122**: 270–280.
- Whitfield, T., M. Granato, F. van Eeden, U. Schach, M. Brand, M. Furutani-Seike, P. Haffter, M. Hammerschmidt, C.-P. Heisenberg, Y.-J. Jiang, D. Kane, R. Kelsh, M. Mullins, J. Odenthal, and C. Nüsslein-Volhard. 1996. Mutations affecting development of the zebrafish inner ear and lateral line. *Development* **123**: 241–254.
- Winslow, J., P. Moran, J. Valverde, A. Shih, J. Yuan, S. Wong, S. Tsai, A. Goddard, W. Henzel, F. Hefti, K. Beck, and I. Caras. 1995. Cloning of AL-1, a ligand for an Eph-related tyrosine kinase receptor involved in axon bundle formation. *Neuron* **14**: 973–981.
- Wood, A. and P. Thorogood. 1994. Patterns of cell behaviour underlying somitogenesis and notochord formation in intact vertebrate embryos. *Dev. Dyn.* **201**: 151–167.
- Xu, Q., G. Alldus, N. Holder, and D.G. Wilkinson. 1995. Expression of truncated Sek-1 receptor tyrosine kinase disrupts the segmental restriction of gene expression in the *Xenopus* and zebrafish hindbrain. *Development* **121**: 4005–4016.
- Xu, Q., G. Alldus, R. Macdonald, D. Wilkinson, and N. Holder. 1996. Function of the Eph-related receptor tyrosine kinase gene *rtk1* is required for regional specification in the zebrafish forebrain. *Nature* **381**: 319–322.